Desalination and Water Treatment
www.deswater.com
1944-3994/1944-3986 © 2012 Desalination Publications. All rights reserved
doi: 10/5004/dwt.2012.2443

Taylor & Francis
Taylor & Francis Group

42 (2012) 8–16
April

Optimizing the sparging condition and membrane module spacing for a ZW500 submerged hollow fiber membrane system

Blair G. Fulton, Pierre R. Bérubé*

Department of Civil Engineering, University of British Columbia, Vancouver, Canada, V6T 1Z4
Tel. +1604 822-5665; Fax: +1604822-6901; email: berube@civil.ubc.ca

Received 20 October 2010; Accepted 26 June 2011

ABSTRACT

The present study characterized the surface shear forces induced by sparging for different sparging conditions (i.e. continuous, alternating and pulse) and the membrane module configurations (i.e. spacing). The root mean square (RMS) of surface shear forces induced by gas sparging, which has been reported to be related to the extent of fouling control in membrane systems, were relatively similar for continuous, alternating and pulse sparging. Considering that pulse sparging uses approximately half of the volume of sparged gas than continuous or alternating sparging, the results suggest that pulse sparging is the best sparging approach. The RMS of surface shear forces were substantially higher for the wide module spacing than for the standard (i.e., narrow) module spacing, indicating that fouling control can likely be significantly improved by simply increasing the distance between the membrane modules.Because of the heterogeneous distribution of surface shear forces and sparged bubbles, it is essential to consider the hydrodynamic conditions throughout the system, rather than just those at the periphery, to optimize the sparging conditions and the module spacing.

Keywords: Fouling control; Hollow fiber membranes; Membrane module spacing; Sparging conditions; Submerged hollow fiber; Surface shear forces

1. Introduction

Ultrafiltration membranes are increasingly being used for both water and wastewater treatment applications because of their ability to effectively remove particulate contaminants of interest. However, these retained contaminants can accumulate at the membrane surface increasing the resistance to the permeate flow. Gas sparging is commonly used in submerged membrane systems to induce shear forces at the membrane surface, which effectively remove the accumulated foulants [1].

In a recent study, the sparged bubble characteristics (i.e. size, rise velocity, count) and the induced shear forces at the surface of submerged hollow fiber membranes were characterized for commercial scale ZW500 membrane modules [2]. The results suggested that the relatively narrow gap between the membrane modules in the system prevented the sparged gas from travelling between the modules. To confirm this hypothesis, the present study investigated the effect of membrane module spacing on the distribution of surface shear forces and sparged bubbles in a ZW500 system with commercial scale membrane modules. The present study also investigated the effect of the sparging conditions (i.e. continuous and intermittent) on the magnitude and distribution of surface shear forces in the system. Intermittent sparging, as opposed to continuous sparging, is increasingly being used in commercial scale submerged

*Corresponding author.

membrane systems. Because the gas flow is interrupted during part of the intermittent sparging cycle, the total volume of gas used for intermittent sparging can be substantially less than that used for continuous sparging. In addition to reducing power costs, empirical results indicate that intermittent sparging does not increase the extent of foulant accumulation, compared to operation with continuous sparging.

2. Experimental approach

A system containing three commercial scale ZeeWeed 500c (hereafter referred to as ZW500 unless otherwise indicated) membrane modules (GE—Water and Process Technologies, Oakville, Canada) was used. Systems with three module cassettes are typically used to pilot ZW500 type systems, as the performance of three module systems, especially in terms of fouling, has been reported to be similar to that of commercial scale systems (M. Theodoulou, 2008, personal communication).

The cassette frame provided by GE was modified to include pneumatic actuators that enabled the spacing between the membrane modules to be remotely varied without having to remove the cassette from the pilot system tank. Two membrane module spacing were considered in the present study: 6.35 and 12.3 cm between membrane module centerlines. The 6.35 cm spacing corresponds to that of the standard ZW500 system, while the 12.3 cm spacing corresponds to the maximum spacing that could be accommodated in the cassette frame and system tank. A picture of the membrane modules in the cassette frame is presented in Fig. 1(a). Sparging was provided via two coarse bubble diffusers, made from 2.5 cm diameter piping with 0.5 cm diameter holes fixed to the base of the cassette, approximately 0.2 m below the membrane modules. Nitrogen was used for gas sparging, as oxygen can affect the performance of the electrochemical method used to measure surface shear forces [3]. To minimize the volume of nitrogen used during the study, a rotary vane pump was used to recirculate the gas in the headspace of the sealed system tank for gas sparging. A condenser/liquid separator and gas drier (i.e. silica gel column) removed moisture from the gas recirculated from the headspace to prevent moisture from disrupting the operation of the pump. The sparging flow rate was set to 10.2 $m^3 h^{-1}$ (0.17 $m^3 m^{-2}$ of membrane area), and monitored using a rotameter, with the pump flow rate controlled using a variable frequency drive. Both continuous and intermittent (alternating and pulse) sparging conditions were investigated. For alternating sparging, the gas flow was either sent to the diffuser located under module 1 or under the module 3, in an alternating sequence. For pulse sparging, gas flow was either sent to both diffusers, or none. At a given sparging flow rate, pulse sparging provided approximately half of the volume of sparged gas as that used for continuous or alternating sparging, while alternating sparging provided approximately twice the flow of sparged gas to each diffuser as that used for continuous or pulse sparging. Fast (6-s cycle: 3 s on and 3 s off) and slow (12 s cycle: 6 s on and 6 s off) intermittent sparging frequencies were considered. The system tank was 2.16 m high, 0.85 m wide and 0.47 m in length. The cassette was located in the system tank, with a spacing of approximately 1–3 cm between the cassette frame and the inside walls of the system tank on all sides. The system tank was filled with RO water, to which the electrolytes needed for the surface shear force measurements or bubble characterization were added [2], and the temperature of the solution was monitored and maintained at 16.5°C. A summary of all of the experimental conditions investigated (i.e. different membrane module spacings and sparging conditions) is presented in Table 1. A randomized factorial experimental design approach was used to investigate the effect of the different experimental conditions on surface shear forces and bubble characteristics. Each experimental condition was repeated three times, each 1 min in duration (note that the first 10 s and last 5 s of each minute were not used for the analysis presented below). In addition, 15 experimental blanks were performed where no sparging was applied. These experiments were performed without interruption over a period of 42 h. Note that

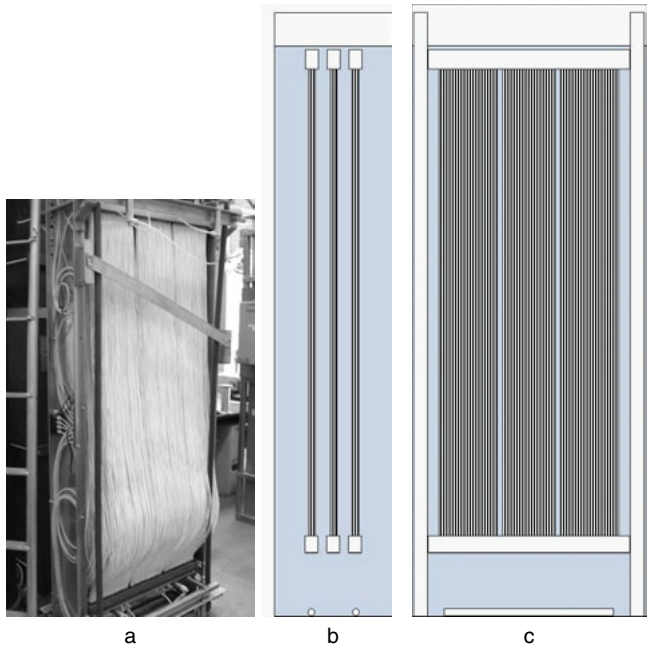

Fig. 1. Picture and schematic of pilot system, spargers and membrane modules. (a): Picture; (b) side view schematic; and (c) front view schematic.

Table 1
Experimental conditions investigated

Experimental condition	Description	Set-point
Module spacing	Standard[1]	6.35 cm between membrane module centerlines
	Wide	12.30 cm between membrane module centerlines
Sparging condition	Continuous	To both diffusers
	Intermittent	Alternating between the two diffusers • Fast alternating: 6 s cycles (3 on and 3 off) • Slow alternating: 12 s cycles (6 on and 6 off)
		Pulse on and off to both diffusers • Fast alternating: 6 s cycles (3 on and 3 off) • Slow alternating: 12 s cycles (6 on and 6 off)

[1]Standard ZW500c configuration.

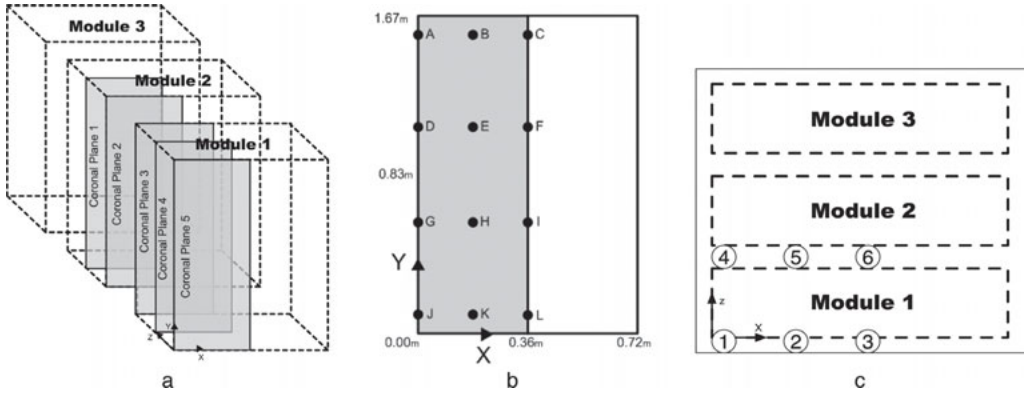

Fig. 2. Location of surface shear force and bubble characteristic measurements. (a) Coronal planes within shaded quarter of interest; (b) locations where shear forces were measured on each coronal plane (rows ABC, DEF, GHI, and JKL at 'y' of 1.57, 1.08, 0.59, and 0.10 m, respectively, and columns ADGJ, BEHK and CFIJ at 'x' of 0, 0.18 and 0.36 m, respectively); (c) locations where bubble characteristics were assessed (locations 1, 2 and 3, as well as 4, 5, and 6, at 'x' of 0, 0.18 and 0.36 m, respectively).

throughout the study, the system was operated without any permeation through the membranes. However, it should be noted that for the type of system being investigated (i.e. ZW500c), for which the permeate flux is typically in the order of 20–50 l m^{-2}·h^{-1} for wastewater and drinking water applications, respectively, and the bulk liquid velocity at the membrane surface is typically greater than 0.1 m s^{-1} [2], the suction rate (defined as ratio of uniform suction velocity to bulk inlet velocity) is less than 0.01%, and therefore the effect of permeation on the hydrodynamic conditions at the membrane surface is expected to be negligible [4,5].

Because the cassette within the system tank was symmetrical about two vertical axes, the surface shear forces and bubble characteristics were only characterized for one quarter of the system, as illustrated in Fig. 2(a). The surface shear forces were characterized for five coronal planes. Within each of the planes, surface shear forces were measured at 12 locations, as presented in Fig. 1(b) (i.e. at a total of 60 locations within the system). The sparged bubbles were characterized at 6 locations near the top of the liquid surface at the side (i.e. locations 1–3 in Fig. 2(c)) and between (i.e. locations 4–6 in Fig. 2(c)) the membrane modules.

The surface shear forces were measured using an electrochemical method. With this approach, the shear forces at a surface can be estimated based on the diffusion limited current passing from a cathode to an anode, through a solution, containing a reversible ion couple [6]. Cathodes, hereafter referred to as shear probes, made from 0.5 mm diameter platinum wire, were embedded flush to the outer surface of Teflon® tubes, hereafter referred to as test fibers, of similar diameter and flexibility to ZW500 hollow fibers (Fig. 3(a)). A total of 60 test fibers were made, each with one shear probe, and were placed within the membrane modules such that the location of the shear probes corresponded to the measurement locations illustrated in Figs. 2(a) and 2(b). The characteristics

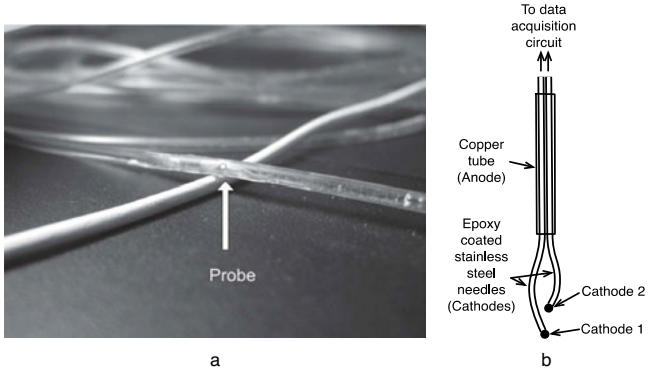

Fig. 3. Shear probe and conductivity micro-probe. (a) Test fiber resting on ZW500 hollow fiber; (b) schematic of conductivity micro-probe.

of the sparged bubbles were determined using two conductivity probes with vertically aligned cathodes (Fig. 3(b)). With this approach, the count, the rise velocity and the size of sparged bubbles can be estimated based on the number of times the signal from either conductivity probe is interrupted, the time lag for both conductivity probes to be interrupted (i.e. flight time), and the duration of the interruption, respectively. Additional details of the approaches used to measure the surface shear forces and to characterize the sparged bubbles, as well as the quality assurance and control procedures used, are presented in Fulton et al. [2].

3. Results and discussion

Typical surface shear forces measured at different locations in the cassette for continuous, pulse and alternating sparging conditions are presented in Figs. 4–6, respectively. For all conditions investigated, the surface shear forces were highly variable over time, ranging from approximately 0 to over 10 Pa. The baseline surface shear forces (i.e. minimum values) were likely induced by the bulk liquid movement within the system tank, while the peak shear events were likely induced by the

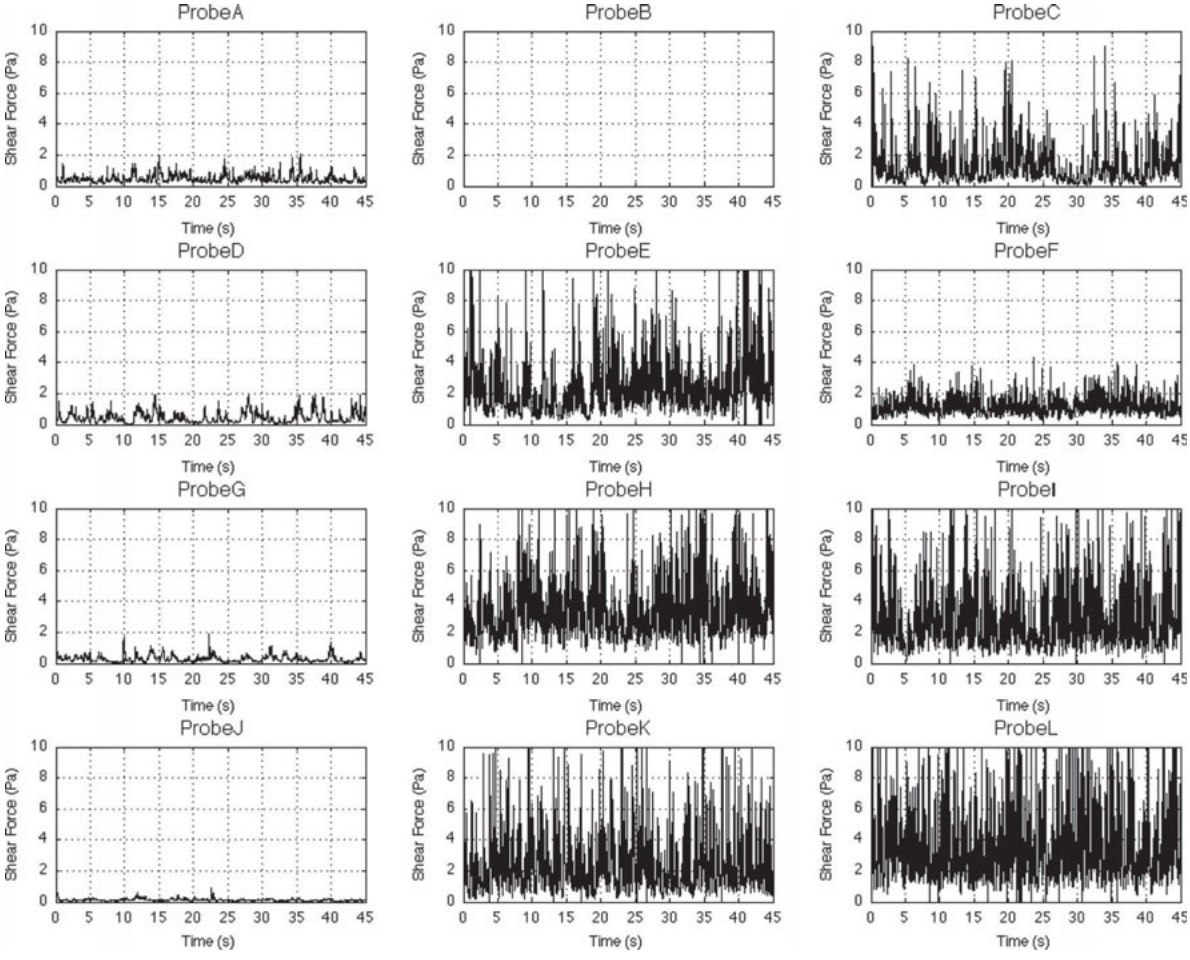

Fig. 4. Typical surface shear forces over time for continuous sparging conditions (results presented are for wide module spacing and coronal plane 3; probe B did not function properly and was omitted from the analysis; refer to Fig. 2 for a description of the probe and plane location within the cassette).

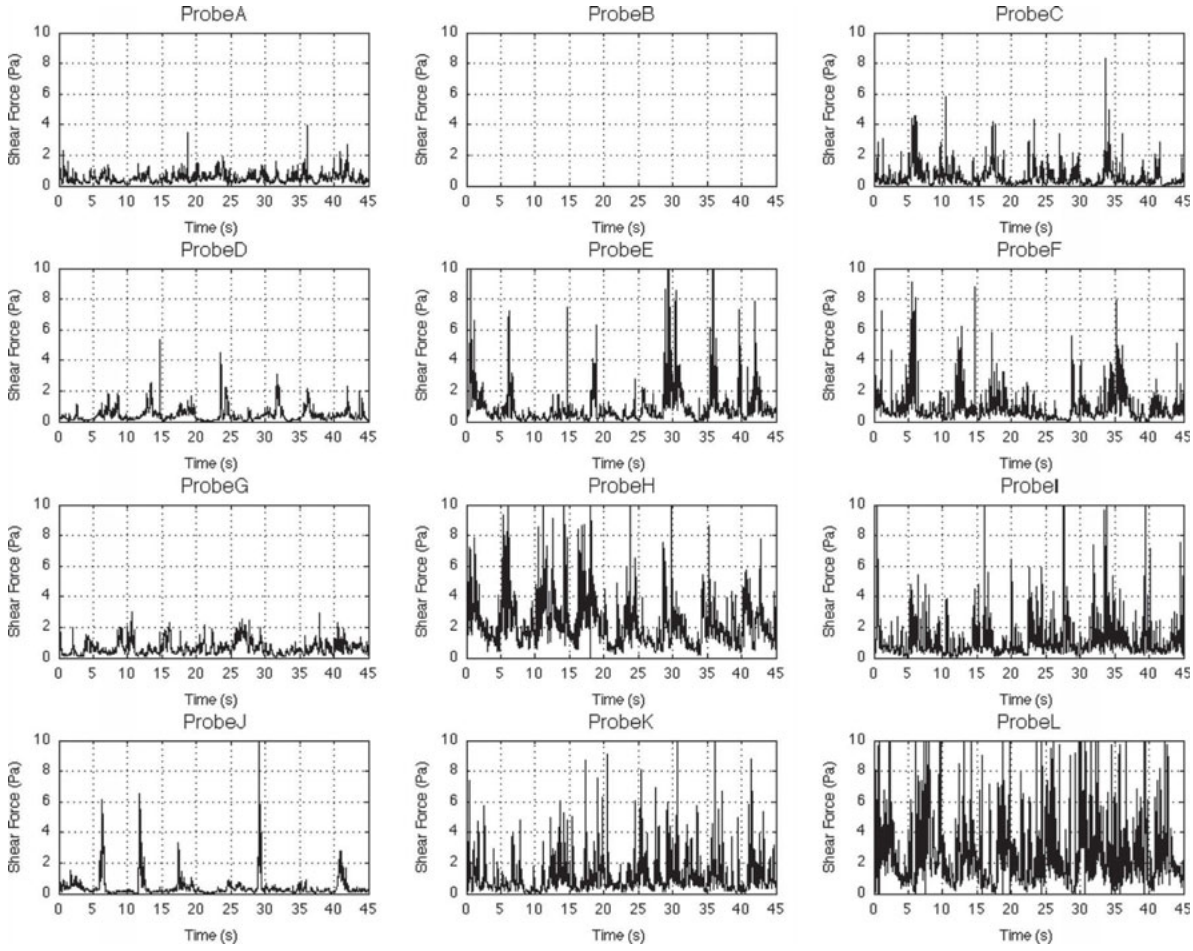

Fig. 5. Typical surface shear forces over time for pulse sparging conditions (results presented are for slow frequency wide module spacing and coronal plane 3; probe B did not function properly and was omitted from the analysis; refer to Figs. 2(a) and 2(b) for a description of the probe and plane location within the caesette).

passage of gas bubbles in proximity to the probe surfaces [7]. In contrast with continuous sparging (Fig. 4), extended periods of high or lower surface shear forces were observed for intermittent sparging (Figs. 5 and 6), especially for slow intermittent sparging frequencies. This was somewhat expected as sparging is repeatedly interrupted during the intermittent sparging conditions. The periods of high or low shear forces were much less distinct for pulse (Fig. 5) than for alternating (Fig. 6) sparging, indicating that for pulse sparging, the surface shear forces were not rapidly dampened when the sparging gas flow was turned off.

Although the relationship between surface shear forces and fouling controls remain unclear, statistically significant correlations have been reported between the root mean square (RMS) of surface shear forces over time induced by gas sparging and the extent of fouling in membrane systems [8,9]. For this reason, in the discussion that follows, the results are presented in terms of RMS of the surface shear forces.

As presented in Table 2, both the sparging conditions and the module geometry affected the cassette RMS of surface shear forces (i.e. for all probes in cassette). In general, the cassette RMS was lowest for continuous sparging and highest for alternating sparging, however the differences were relatively small and not consistently statistically significant. Also, there was no significant difference between the cassette RMS of surface shear forces induced by intermittent sparging at different frequencies. On the other hand, the cassette RMS of surface shear forces were significantly higher for the wide module spacing compared to the standard module spacing. These results suggest that greater fouling control can likely be achieved by simply widening the spacing between the membrane modules. Also, pulse sparging can achieve similar levels of fouling control as continuous and alternating sparging, but with half the volume of sparged gas.

The distribution of RMS of surface shear forces in the cassette (i.e. for individual probes locations in cassette)

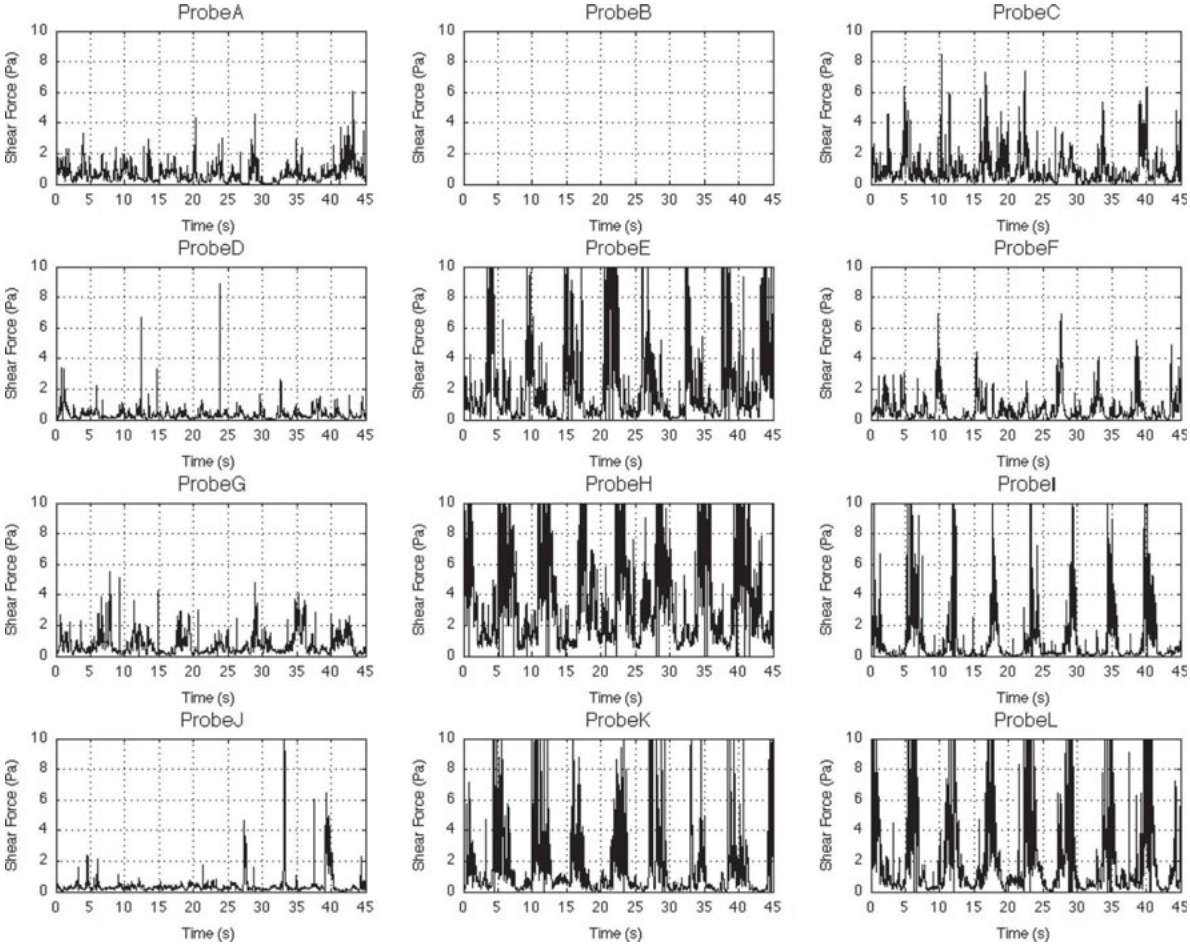

Fig. 6. Typical surface shear forces over time for alternating sparging conditions (results presented are for slow frequency, wide module spacing and coronal plane 3; probe B did not function properly and was omitted from the analysis; refer to Figs. 2(a) and 2(b) for a description of the probe and plane location within the cassette).

Table 2
RMS of surface shear forces in the cassette

Sparging conditions	Intermittent frequency	Module spacing	RMS of surface shear forces in the cassette[2] (Pa)
Continuous	–	Standard[1]	0.34 ± 0.15
		Wide	0.94 ± 0.21
Alternating	Slow	Standard[1]	0.64 ± 0.04
		Wide	1.27 ± 0.04
	Fast	Standard[1]	0.63 ± 0.40
		Wide	1.20 ± 0.13
Pulse	Slow	Standard[1]	0.47 ± 0.01
		Wide	0.88 ± 0.06
	Fast	Standard[1]	0.52 ± 0.34
		Wide	0.93 ± 0.09

[1]Corresponds to module geometry for standard ZW500c system.
[2]Values presented are averages of replicate experiments ± 90% confidence interval of replicate experiments.

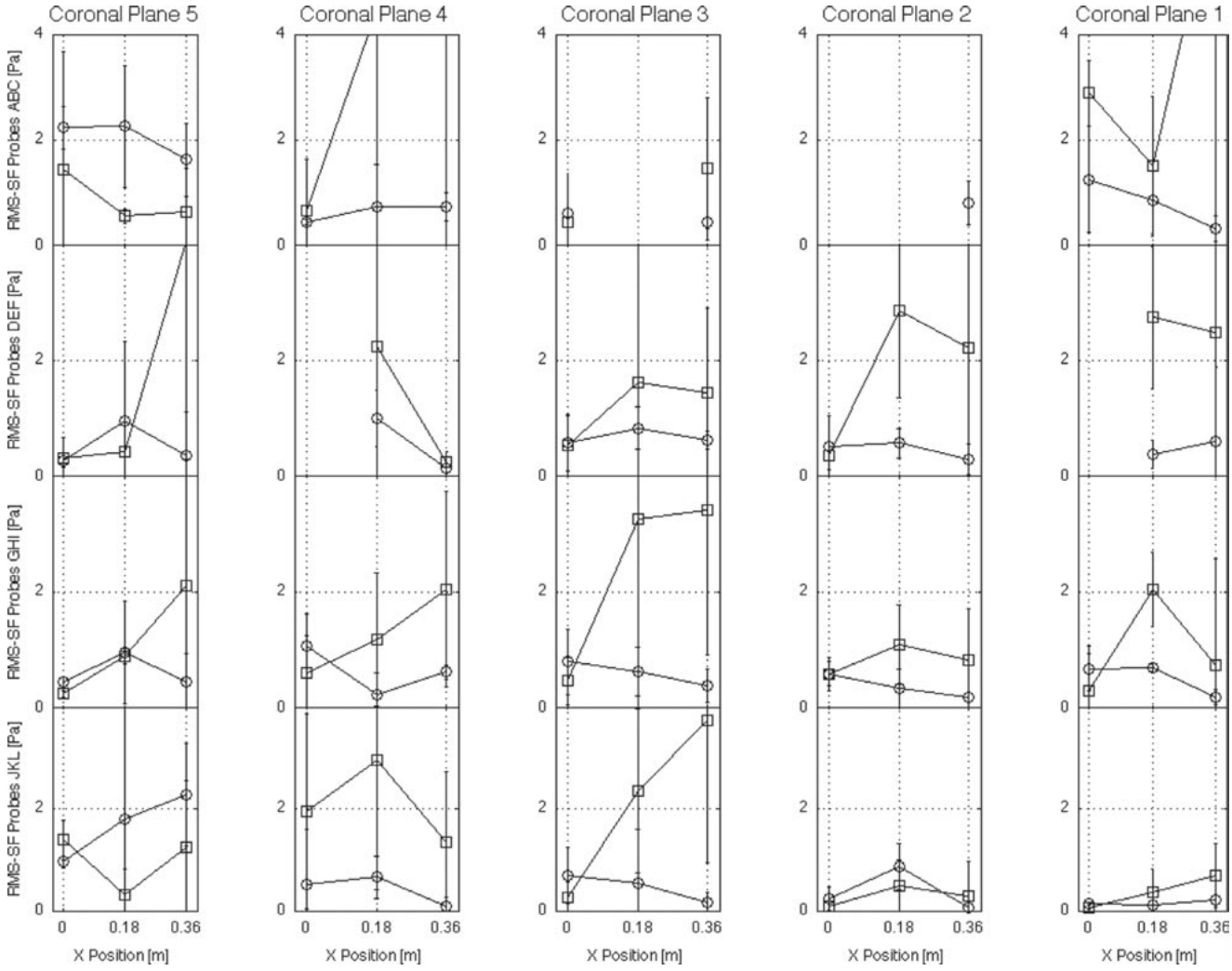

Fig. 7. Distribution of RMS of surface shear forces for standard and wide module spacing (O: standard module spacing; □: wide module spacing; results presented are for continuous sparging, similar results were observed for alternating and pulse sparging at fast and slow intermittent frequencies; values presented are averages of replicate experiments ±90% confidence interval of replicate experiments; refer to Figs. 2(a) and 2(b) for a description of the probe and plane location within the cassette).

was relatively similar for the different sparging conditions investigated (results not presented). For this reason, in the discussion that follows, only the results for continuous sparging conditions are presented. The module spacing, on the other hand, significantly affected the distribution of RMS of surface shear forces (Fig. 7). For the standard module spacing, with the exception of the higher magnitude observed at the base of coronal plane 5, the RMS of surface shear forces were relatively homogeneously distributed throughout the cassette and generally less than 1 Pa. For the wide module spacing, the RMS of surface shear forces were heterogeneously distributed. At the edge of the modules (i.e. X position 0 m), the RMS of surface shear forces were similar to those observed for the standard module spacing, while within the modules (X position 0.18 and 0.36 m), the RMS of surface shear forces were generally higher, resulting in cassette RMS of surface shear forces that were greater for the wide module spacing than for the standard module spacing.

As presented in Fig. 8, the distribution of bubble counts was significantly affected by the module spacing. For the standard module spacing, the bubble count at the side of the modules was higher than between the membrane modules. Widening the distance between the membrane modules significantly increased the bubble counts between the membrane modules, and reduced those at the side of the modules.

These results confirm that the hypothesis formulated by Fulton et al., which suggested that the relatively

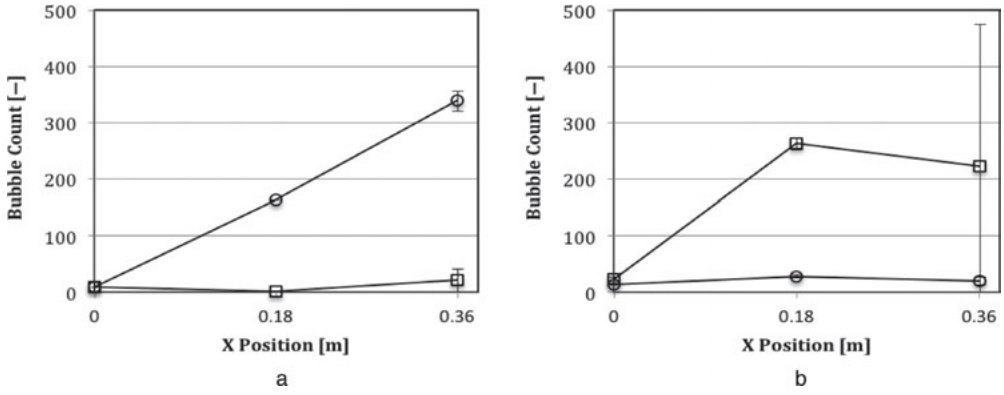

Fig. 8. Distribution of bubble counts. (a) Side of membrane modules, (b) between membrane modules; ○: standard module spacing; □: wide module spacing; values presented are averages of replicate experiments ±90% confidence interval of replicate experiments; results presented are for continuous sparging; 'X' positions of 0, 0.18 and 0.36 m corresponds to locations 1, 2 and 3, respectively, at the side of the membrane modules, and 4, 5, and 6, respectively, between the membrane modules; refer to Fig. 2(c) for description of measurement locations within the cassette).

narrow gap between the membrane modules in the standard ZW500c system prevented the sparged gas from rising between the modules [2]. It is likely that the higher number of sparged bubbles that rose between the membrane modules for the wider module spacing contributed to the greater RMS of surface shear forces observed for the wider module spacing. The lower bubble counts at the edge of the membrane modules (i.e. X position 0 m), compared to those within the membrane modules (i.e. X position 0.18 and 0.36 m), is consistent with results of other studies that have reported that sparged bubbles tend to migrate towards the centerline of the membrane modules as they rise [2,10]. This lateral migration is likely responsible for the lower surface shear force magnitudes observed at the edges of the membrane modules (i.e. at probe locations A, D, G and J in Figs. 4–6), compared to those within the membrane modules (i.e. at probe locations B, C, E, F, H, I, K and L in Figs. 4–6). It should however be noted that no correlation was observed between the bubble count and the RMS of surface shear forces (results not presented), which is consistent with results from a previous study [2]. The lack of a direct correlation is likely because the surface shear forces induced on the hollow fibers by gas sparging are not only affected by the count of the sparged bubbles, but also by entrained bulk liquid flow, local liquid instabilities and fiber sway [8,11].

Because of the heterogeneous distribution of surface shear forces and sparged bubbles, it is essential to consider the hydrodynamic conditions throughout the system, rather than just those at the periphery, to optimize the sparging conditions and the module spacing.

The results from the present study are expected to be valid for ZW500 type systems containing Newtonian fluids such as water or mixed liquor. The surface shear forces are expected to be different for systems containing non-Newtonian fluids such as mixed liquors with high suspended solids concentrations [12].

4. Conclusions

The surface shear forces were observed to be highly variable over time and heterogeneously distributed within the cassette. In contrast with continuous sparging, extended periods of high or lower surface shear forces were observed for alternating and pulse sparging.

The root mean square (RMS) of surface shear forces induced by gas sparging, were relatively similar for continuous, alternating and pulse sparging, even though the volume of gas used by pulse sparging was half of that used by the other sparging conditions. Increasing the distance between the membrane modules significantly increased the cassette RMS of surface shear forces, suggesting that fouling control can improved by simply widening the distance between the membrane modules. It is likely that the greater number of sparged bubbles that could rise between the wider spaced membrane modules contributed to the higher RMS of surface shear forces. Because of the heterogeneous distribution of surface shear forces and sparged bubbles, it is essential to consider the hydrodynamic conditions throughout the system, rather than just those at the periphery, to optimize the sparging conditions and the module spacing.

The approach developed to map the surface shear forces throughout a sparged submerged hollow fiber membrane systems provided the information needed to maximize surface shear forces without having to rely on a time and capital intensive trial-and-error approach.

Acknowledgements

Funding for this study was provided by GE Water and Process technologies and the Natural Sciences and Engineering Research Council of Canada.

References

[1] Z.F. Cui, S. Chang and A.G. Fane, The use of gas bubbling to enhance membrane processes, J. Membr. Sci., 221(1–2) (2003) 1–35.
[2] B. Fulton, J. Redwood, M. Tourais and P.R. Bérubé, Distribution of surface shear forces and bubble characteristics in full-scale gas sparged submerged hollow fiber membrane modules, Desalination, 281 (2011) 128–141.
[3] F.R. Berger and A. Ziai, Optimization of experimental conditions for electrochemical mass transfer measurements, Chem. Eng. Res. Des., 61(6) (1983) 377–382.
[4] D. Sofialidis and P. Primos, Fluid flow and heat transfer in a pipe with wall suction, Int. J. Heat Mass Trans., 40(15) (1997) 3627–3640.
[5] H. Tennekes, Similarity laws for turbulent boundary layers with suction and injection, J. Fluid Mech., 21 (1965) 689–703.
[6] L.P. Reiss and T.J. Hanratty, Measurement of instantaneous rates of mass transfer to a small sink on a wall, AICHE J., 8(2) (1962) 245–247.
[7] C.C.V. Chan, P.R. Bérubé and E.R. Hall, Shear profiles inside gas sparged submerged hollow fiber membrane modules, J. Membr. Sci., 297(1–2) (2007) 104–120.
[8] C.C.V. Chan, P.R. Bérubé and E.R. Hall, Relationship between types of surface shear stress profiles and membrane fouling, J. Water Res., 45(19) (2011) 6403–6416.
[9] A.P.S. Yeo, A.W.K. Law and A.G. Fane, The relationship between performance of submerged hollow fibers and bubble-induced phenomena examined by particle image velocimetry, J. Membr. Sci., 304 (2010) 125–137.
[10] E. Nguyen Cong Duc, L. Fournier, C. Levecq, B. Lesjean, P. Grelier and A. Tazi-Pain, Local hydrodynamic investigation of the aeration in a submerged hollow fiber membrane cassette, J. Membr. Sci., 321(2) (2008) 264–271.
[11] F. Wicaksana, A.G. Fane and V. Chen, Fiber movement induced by bubbles using submerged hollow fiber membranes, J. Membr. Sci., 271 (2006) 186–195.
[12] N. Ratkovich, P.R. Bérubé and I. Nopens, Assessment of mass transfer coefficients in coalescing slug flow in vertical pipes and applications to tubular airlift membrane bioreactors, Chem. Eng. Sci., 66(6) (2011) 1254–1268.